

# Parametric Projection Operator Technique for Second Order Non-linear Response

Jan Olšina and Tomáš Mančal

*Faculty of Mathematics and Physics, Charles University in Prague,  
Ke Karlovu 5, CZ-121 16 Prague 2, Czech Republic*

We demonstrate the application of the recently introduced parametric projector operator technique to a calculation of the second order non-linear optical response of a multilevel molecular system. We derive a parametric quantum master equation (QME) for the time evolution of the excited state of an excitonic system after excitation by the first two pulses in the usual spectroscopic four-wave-mixing scheme. This master equation differs from the usual QME by a correction term which depends on the delay  $\tau$  between the pulses. In the presence of environmental degrees of freedom with finite bath correlation time and in the presence of intramolecular vibrations we find distinct dynamics of both the excited state populations and the electronic coherence for different delays  $\tau$ .

## I. INTRODUCTION

Recent years have seen a rapid experimental development in multidimensional coherent spectroscopy. Developed first in the nuclear magnetic resonance [1] it has been brought to infra red [2–4] and later into near infra-red and optical domains [5, 6]. Since then it yielded new insights into photo-induced dynamics of electronic excited states of small molecules [7], polymers [8], large photosynthetic aggregates [9, 10] and even solid state systems [11]. The two-dimensional (2D) Fourier transformed spectrum completely characterizes the third order non-linear response of a molecular ensemble in amplitude and phase [12, 13] providing thus, the maximal information accessible in a three pulse experiment. In the three pulse degenerate four wave mixing (FWM) experiment [14], two independent adjustable parameters – the delays between the three pulses – allow experimentalists to address the time and delay dependent third order non-linear response of the molecular system  $S^{(3)}(t, T, \tau)$  via complete characterization of the third order non-linear signal  $E_s^{(3)}(t, T, \tau)$  (see Fig. 1). This information is conveniently represented by a 2D plot of the Fourier transformed signal  $E_s^{(3)}(\omega_t, T, \omega_\tau)$  which correlates the absorption frequency  $\omega_\tau$  with the frequency  $\omega_t$  of stimulated emission, ground state bleaching and excited state absorption contributions, separated from the absorption event by an adjustable waiting time  $T$ . Femtosecond photo-induced evolution of molecular systems is reflected in the amplitude, position and shape of 2D spectral features as functions of the waiting time revealing thus important information about the molecular structure, intramolecular dynamics, as well as the interaction of molecular electronic transitions with their environment [15–17].

By analyzing 2D spectra of photosynthetic Fenna-Mathews-Olson (FMO) protein, Brixner et al. have first demonstrated the ability of the new technique to improve our knowledge of energy transfer pathways in photosynthetic proteins [15, 18]. Later, signatures of electronic quantum coherence in this system have been theoretically predicted [16] and experimentally verified [9]. The

same measurements led to a surprising discovery of the long life time of these electronic coherence and to an identification of a host of other effects which contribute to the wave-like nature of the energy transfer in these systems. Recently, coherent oscillations in 2D spectra of photosynthetic systems were demonstrated even for room temperature [19, 20]. The impact of these new finds has been felt well beyond the photosynthesis research community, and the quantum properties of energy transfer in biological systems have attracted researches from seemingly unrelated fields of quantum computation and quantum information science. Questions about the relevance of quantum effects in natural light harvesting have led researches to study quantum entanglement [21–23], various aspects of the environmental assistance in quantum transport and optimality of transport processes [24–28]. Meanwhile, measurement of electronic coherence have found utility in determining structure-related properties of photosynthetic systems. Thus, the electronic beating of 2D spectra have been recently used to precisely determine electronic energy levels in congested spectra of molecular aggregates [29].

In order to yield the above discussed impressive results, optical 2D experiments have to be accompanied by a thorough analysis, which requires detailed theoretical understanding of the molecular response to exciting light. For the description of the most 2D experiments, the third order semi-classical light-matter interaction response function theory is well established. Response functions of model few-level systems with pure dephasing (i.e. with no energy transfer between the levels) can even be expressed analytically in terms of the so-called energy gap correlation function (EGCF), using the second order cumulant in Magnus expansion [14]. Some examples of small chromophores in solution fall in this category [30, 31] when investigated on time scales shorter than radiative life time. For a Gaussian bath this analytical theory is exact, and thus knowing the EGCF of the electronic transitions enables us to determine linear (absorption) as well as non-linear spectra.

However, the construction of exact response functions for realistic energy transferring systems, such as Frenkel excitons in photosynthetic aggregates [32], is

no longer possible. Photosynthetic complexes are relatively large, and the proper methods to simulate finite timescale stochastic fluctuations at finite temperatures [33–35] carry a substantial numerical cost. Practical calculations thus require some type of reduced dynamics where only electronic degrees of freedom (DOF) are treated explicitly. These approaches usually rely on a host of approximations that seem to work well for most spectroscopic techniques [36–39] and in systems where the details of system-bath coupling are apparently less important [40]. With increasing details of the excited state dynamics revealed by the 2D spectroscopy [41–43] and with increasing size of the studied systems, it becomes more and more important to keep the numerical cost of simulations low, while simultaneously account for experimentally observed quantum effects. One of the possible research directions is to extend on existing reduced density matrix (RDM) theories [44, 45] or relax certain approximations [46].

It was demonstrated that RDM master equations derived by projection operator technique reproduce exactly the linear response [47]. In the case of higher order response functions, however, the same approach necessarily neglects bath correlations between the different periods of photo-induced system evolution (i.e. between so-called coherence time  $\tau$  and the waiting time  $T$ ). The failure to account for this correlation leads sometimes to a complete loss of the experimentally observed dynamics in simulated 2D spectra, such as in the case of the vibrational modulation of electronic 2D spectra [30]. Because vibrational modulation leads to effects similar to those attributed to electronic coherence, developing methods that can account for its effect reliably in complex systems is of utmost importance. One possible approach to the problem is to derive equations of motion for the response as a whole, and to take the previous time evolution of the system into account explicitly [48]. In this paper, we take a different route in which the correlation effects are treated by a specific choice of the projection operator. Once a projector is specified, it can be used for any method of treating system bath interaction. We apply the previously suggested parametric projection operator technique [49] to a calculation of the second order response of a quantum system. The second order response operators can be used to determine the state of a molecular system subject to excitation by a weak light with arbitrary properties, and thus its importance goes beyond the semi-classical system light interaction theory [50]. Alternatively, calculation of the second order response can be viewed as a first step towards more involved calculation of the third order response functions that is required for the modeling of the third order non-linear spectra.

The paper is organized as follows: in the next section we specify the model Hamiltonian and the description of the system's interaction with the light and its environment (the thermodynamic bath). In Section III we discuss the third order response functions of a multilevel

systems, and we point out general limitations of their evaluation by the reduced density matrix master equations. In Section IV we write out the density operator describing the excited state of a molecular system in terms of the second order response operator, and we discuss the advantages of usage of the parametric projection operator over the standard projectors. The details of the parametric projection operator and the corresponding master equation are introduced in Section V. Numerical results for the excited state dynamics are then discussed in Section VI. Some definitions and calculation details can be found in the Appendices.

## II. MODEL SYSTEM AND BLOCK FORMALISM

Our primary interest lies in photosynthetic aggregates of chlorophylls. Frenkel exciton model is well established for the description of photosynthetic systems and their spectroscopy [15, 32]. The second order response, which we have in mind here, corresponds to the interaction of the excitonic system with first two pulses in a standard FWM spectroscopy (see Fig. 1), and it should correspondingly describe the time evolution of the system in the excited or ground state. The part of the response associated with evolution in the excited state also corresponds to the material quantities that govern excitation of molecular systems by arbitrary quantum light [50].

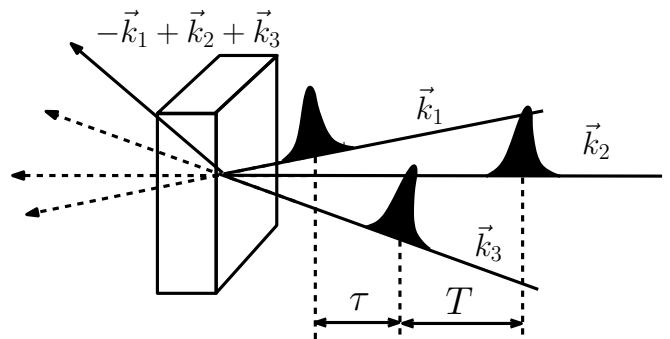


Figure 1: A scheme of a typical FWM experiment. Three laser pulses with delays  $\tau$  and  $T$  are incident on a sample. A non-linear signal generated into a selected direction,  $-\vec{k}_1 + \vec{k}_2 + \vec{k}_3$  here, is detected.

For a second order response we need to consider only single exciton band, i.e. the collective excited states of the aggregate with only a single aggregate member excited. The Frenkel Hamiltonian including environmental contributions has the general form  $H = H_S + H_B + H_{S-B}$ , where the purely electronic (system) Hamiltonian  $H_S$  reads

$$H_S \equiv \varepsilon^g |g\rangle\langle g| + \sum_n (\varepsilon^n + \langle \Phi_n^e - \Phi^g \rangle) |n\rangle\langle n|$$

$$+ \sum_{mn} j_{mn} |m\rangle\langle n|, \quad (1)$$

the bath Hamiltonian  $H_B$  can be identified with

$$H_B \equiv T + \Phi^g, \quad (2)$$

and the system-bath interaction  $H_{S-B}$  reads as

$$H_{S-B} \equiv \sum_n \Delta\Phi_n |n\rangle\langle n|. \quad (3)$$

Here,  $|g\rangle$  is the electronic ground state of the aggregate of molecules with energy  $\varepsilon^g$ ,  $|m\rangle$  are electronic states with the  $m^{\text{th}}$  molecule of the aggregate of  $N$  molecules excited with energy  $\varepsilon^n$ ,  $j_{nm}$  represents resonance coupling between excited states  $|m\rangle$  and  $|n\rangle$ ,  $\Phi$  represents potential energy surfaces (PES) of the bath DOF in corresponding electronic states, and  $T$  is the kinetic energy of the bath DOF. We also defined so-called energy gap operator

$$\Delta\Phi_n \equiv \Phi_n^e - \Phi^g - \langle \Phi_n^e - \Phi^g \rangle, \quad (4)$$

where  $\langle \bullet \rangle$  represents the equilibrium quantum mechanical average over the bath DOF. Symbol  $\bullet$  denotes an arbitrary operator. The interaction of the system with light will be described by the usual semi-classical light-matter interaction term in dipole approximation

$$H_{S-E}(t) = -\boldsymbol{\mu} \cdot \mathbf{E}(t). \quad (5)$$

Here,  $\boldsymbol{\mu}$  is the transition dipole moment operator of the aggregate system and  $\mathbf{E}(t) = \mathbf{e}E(t)$  is the electric field vector of the light with polarization vector  $\mathbf{e}$ .

The states  $|m\rangle$  with excitations localized on individual member molecules of the aggregate allow us to define the properties of the aggregate based on crystal structure and quantum chemical inputs. It is, however, often more convenient to work in a basis of the eigenstate  $|\tilde{m}\rangle$  of the electronic Hamiltonian  $H_S$ . For later convenience we will define projection operators  $K_m = |m\rangle\langle m|$  projecting on a state in the local basis and  $K_{\tilde{m}} = |\tilde{m}\rangle\langle \tilde{m}|$  projecting on the eigenstate (excitonic) basis. For the discussion of the non-linear response functions, it is advantageous to use a superoperator formalism. We define the dipole moment superoperator as

$$\mathcal{V}\bullet = \frac{1}{\hbar} [\boldsymbol{\mu}, \bullet]_- = \frac{1}{\hbar} [\boldsymbol{\mu} \cdot \mathbf{e}, \bullet]_-, \quad (6)$$

and the Liouvillian as

$$\mathcal{L}\bullet = \frac{1}{\hbar} [H, \bullet]_-. \quad (7)$$

We will also use the evolution operator

$$U(t) = \exp\left\{-\frac{i}{\hbar}Ht\right\}, \quad (8)$$

and the evolution superoperator

$$\mathcal{U}(t)\bullet = U(t) \bullet U^\dagger(t), \quad (9)$$

where convenient.

In the second order system-bath coupling theories, the energy gap operators, Eq. (4), are present in the equations via the EGCFs

$$C_{mn}(t) \equiv \langle U^\dagger(t)\Delta\Phi_m U(t)\Delta\Phi_n \rangle. \quad (10)$$

Double integration of  $C_{mn}(t)$  over time yields so-called lineshape functions

$$g_{mn}(t) \equiv \frac{1}{\hbar^2} \int_0^t d\tau \int_0^\tau d\tau' C_{mn}(\tau'), \quad (11)$$

which determine absorption and emission line shapes. Later in the text, it will be convenient to define the energy gap operators in the excitonic basis

$$\Delta\Phi_{\tilde{a}\tilde{b}} = \sum_k \Delta\Phi_k \langle \tilde{a}|k\rangle \langle k|\tilde{b}\rangle, \quad (12)$$

the excitonic EGCFs

$$C_{\tilde{a}\tilde{b}}(t) \equiv \langle U^\dagger(t)\Delta\Phi_{\tilde{a}\tilde{a}} U(t)\Delta\Phi_{\tilde{b}\tilde{b}} \rangle \quad (13)$$

$$= \sum_{kl} |\langle \tilde{a}|k\rangle|^2 |\langle \tilde{b}|l\rangle|^2 C_{kl}(t), \quad (14)$$

and the excitonic lineshape functions

$$g_{\tilde{a}\tilde{b}}(t) \equiv \frac{1}{\hbar^2} \int_0^t d\tau \int_0^\tau d\tau' C_{\tilde{a}\tilde{b}}(\tau'). \quad (15)$$

We are interested in the influence of the bath DOF on the dynamics of the electronic DOF in the excited state. The bath can consist of several types of collective modes which can be described by various types of bath correlation function. Experimental situation is typically well described by one or several overdamped Brownian oscillator modes standing for a macroscopic number of harmonic DOF, and several underdamped oscillator modes standing for some important vibrational coordinates, e.g. normal modes of the chromophore molecules [30]. Both of these limits can be conveniently described by the general Brownian oscillator correlation function  $C(t)$  (see [14]) which is a function of temperature  $T$ , frequency  $\Omega_{\text{Bath}}$  of the oscillator, damping coefficient  $\gamma$  and the reorganization energy  $\lambda$ . In the case of a strongly overdamped mode i.e. when  $\gamma \gg 2\Omega_{\text{bath}}$  the formula simplifies significantly. At high temperatures we have

$$C(t) = \hbar\lambda\Lambda \cot(\Lambda\hbar\beta/2) \exp(-\Lambda t) - i\hbar\lambda\Lambda \exp(-\Lambda t), \quad (16)$$

with  $\Lambda = 1/\gamma$ . In the opposite case of a non-damped oscillator  $\gamma \rightarrow 0$  the correlation function reads

$$C(t) = \lambda\Omega_{\text{Bath}}\hbar \left[ \coth(\beta\hbar\Omega_{\text{Bath}}/2) \cos(\Omega_{\text{Bath}}t) \right]$$

$$-i \sin(\Omega_{\text{Bath}} t)]. \quad (17)$$

The Hamiltonian, Eq. (1), has a block form. In case we would consider excited states with up to  $N$  excitations per aggregate a more general Hamiltonian would have to be written including  $N + 1$  blocks with one block containing just the ground state  $|g\rangle$ , and the  $N$  blocks containing the excited states with one, two,  $\dots$ , up to  $N$  excitations. The block structure is enabled by the fact that the Hamiltonian operators, Eqs. (1) to (3), do not contain any terms that enable de-excitation of excited states. This is a well justified assumption in studies of ultra-fast dynamics of the chlorophyll based photosynthetic aggregates [51]. The transitions between different blocks of the Hamiltonian are only enabled by the interaction with the light, Eq. (5). The second order response, which is of interest in this paper, requires on the ground- and the single-exciton blocks. We will therefore use upper indices  $g$  (ground state) and  $e$  (single exciton block) to denote different blocks of operators and superoperators whenever we are interested in operations on and evolution of their individual blocks. Thus, e.g. the time evolution of the system in excited state single exciton manifold is described by the RDM block  $\rho^{(ee)}(t) = \mathcal{U}^{(eeee)}(t)\rho^{(ee)}(0) = U^{(ee)}(t)\rho^{(ee)}(0)U^{(ee)\dagger}(t)$ , and the action of the dipole operator (superoperator) promotes the ground state block into a coherence block as  $\rho^{(eg)}(t) = \mu^{(eg)}\rho^{(gg)}(t) = \mathcal{V}^{(eggg)}\rho^{(gg)}(t)$ . When working in a particular basis of states (e.g.  $\{|m\rangle\} = \{|1\rangle, |2\rangle, \dots\}$ ) we can write out the sums over the states explicitly, e.g. as

$$\begin{aligned} \rho_{mn}^{(ee)}(t) &= \sum_{kl} \mathcal{U}_{mnkl}^{(eeee)}(t)\rho_{kl}^{(ee)}(0) \\ &= \sum_{kl} U_{mk}^{(ee)}(t)\rho_{kl}^{(ee)}(0)U_{ln}^{(ee)\dagger}(t). \end{aligned} \quad (18)$$

The rules are rooted in the simple well-known fact that matrices can be multiplied by blocks. When discussing the most common non-linear experiments, the block structure has to be considered up to the two-exciton block.

### III. MULTI-POINT CORRELATION FUNCTIONS IN NON-LINEAR SPECTROSCOPY

Non-linear response functions have in general the form of multi-point correlation functions. For a two band system (ground state and single excitons), the third order non-linear spectroscopy is completely described by four response functions [14], listed in Appendix A. As an example, we will consider the response usually denoted as  $R_2$ , Eq. (A2). We can notice that the block (upper) indices of the evolution operators in Eq. (A2) (read from

left to right) follow the double-sided Feynman diagram in Fig. 2A (see [14] for details). During the so-called population interval  $T$  of the response, the system evolves in the excited state band ( $ee$ ). If no resonance coupling is present ( $j_{mn} = 0$  in Eq. (1)) each response function can be split into a sum of independent components. For  $R_2$  this means

$$R_2(t, T, \tau) = \sum_{kl} R_{2,kl}(t, T, \tau), \quad (19)$$

where the components

$$\begin{aligned} R_{2,kl}(t, T, \tau) &= |\mu_{kg}|^2 |\mu_{lg}|^2 \\ &\times \text{tr}_B \{ \mathcal{U}_{kgkg}^{(egeg)}(t) \mathcal{U}_{klkl}^{(eeee)}(T) \mathcal{U}_{glgl}^{(gege)}(\tau) W_{\text{eq}}^{(gg)} \} \end{aligned} \quad (20)$$

can be evaluated analytically in terms of the line shape functions, Eq. (11). Here,  $W_{\text{eq}}^{(gg)} = w_{\text{eq}}|g\rangle\langle g|$  is the total equilibrium density operator (the electronic energy gap is assumed to be much higher than  $k_B T$ ) and  $w_{\text{eq}}$  represents the equilibrium density operator of the bath alone. For  $j_{mn} > 0$  no analytical result is available, and one needs to resort to some master equation simulations of the evolution superoperators  $\mathcal{U}$ . However, the master equations can only deliver certain reduced (i.e. averaged over the state of the bath) version of this superoperator.

The usual way of deriving master equations for the RDM is to apply a projection operator  $\mathcal{P}$  which reduces the full density matrix  $W(t)$  of the system to its selected part [52], in our case, to the electronic DOF

$$\rho(t) = \text{tr}_B \{ W(t) \}. \quad (21)$$

The most popular prescription, the so-called Argyres-Kelly (AK) projector [53], reads as

$$\mathcal{P}_0 W(t) = \rho(t) w_{\text{eq}}. \quad (22)$$

It is easy to see that inserting the identity  $1 = \mathcal{P} + \mathcal{Q}$ , where  $\mathcal{Q} = 1 - \mathcal{P}$  into Eq. (21) leads to

$$\rho(t) = \text{tr}_B \{ \mathcal{U}(t) \mathcal{P} W(0) + \mathcal{U}(t) \mathcal{Q} W(0) \}. \quad (23)$$

Provided that  $\mathcal{Q} W(0) = 0$  (a condition satisfied in the first interval of the response function, Eq. (A2)) one can define the reduced evolution superoperator  $\tilde{\mathcal{U}}(t) = \text{tr}_B \{ \mathcal{U}(t) w_{\text{eq}} \}$  such that  $\rho(t) = \tilde{\mathcal{U}}(t) \rho(0)$ . The evolution superoperator  $\tilde{\mathcal{U}}(t)$  can be calculated from a master equation that can be derived by projection operator formalism [52].

Let us apply the same method to higher order response functions. Let us assume we have derived a master equation by applying the corresponding projector operator  $\mathcal{P}$  and calculated elements of the reduced evolution superoperator  $\tilde{\mathcal{U}}(t)$ . We can then assemble an approximate response function

$$\tilde{R}_{2,kl}(t, T, \tau) = \tilde{\mathcal{U}}_{kgkg}^{(egeg)}(t)$$

$$\times \tilde{\mathcal{U}}_{klkl}^{(eeee)}(T)\tilde{\mathcal{U}}_{glgl}^{(gege)}(\tau)\rho^{(gg)}(0). \quad (24)$$

Here, we set all transition dipole moment elements to one for the sake of brevity. It can be shown that  $\tilde{R}_{2,kl}$  can also be written as

$$\begin{aligned} \tilde{R}_{2,kl}(t, T, \tau) &= \text{tr}_B \{ \mathcal{U}_{kgkg}^{(egeg)}(t) \\ &\times \mathcal{P} \mathcal{U}_{klkl}^{(eeee)}(T) \mathcal{P} \mathcal{U}_{glgl}^{(gege)}(\tau) \rho^{(gg)}(0) \}. \end{aligned} \quad (25)$$

However, the exact expression for  $R_{2,kl}$  reads as

$$\begin{aligned} R_{2,kl}(t, T, \tau) &= \text{tr}_B \{ \mathcal{U}_{kgkg}^{(egeg)}(t) (\mathcal{P} + \mathcal{Q}) \mathcal{U}_{klkl}^{(eeee)}(T) \\ &\times (\mathcal{P} + \mathcal{Q}) \mathcal{U}_{glgl}^{(gege)}(\tau) \rho^{(gg)}(0) \}. \end{aligned} \quad (26)$$

Eqs. (25) and (26) differ by  $\mathcal{Q}$ -containing terms that cannot be in general eliminated, and consequently one cannot expect master equations based on a single projector operator  $\mathcal{P}$  of any type to reproduce the third order response functions. This applies also to the validity of non-perturbative schemes of calculations of non-linear response, such as those derived in Refs. [54] and [55].

A general solution of this problem was proposed in Ref. [49]. It was argued that one cannot write down a single exact master equation for all three intervals of the response function. Rather, one has to write a different master equation for each interval. This is formally possible by introducing three different projectors  $\mathcal{P}_0$  (i.e. standard AK projector) for the first,  $\mathcal{P}_\tau$  for the second and  $\mathcal{P}_{\tau+T}$  for the third interval of the response [49]. The projectors  $\mathcal{P}_\tau$  and  $\mathcal{P}_{\tau+T}$  are constructed so as to cancel the  $\mathcal{Q}$ -containing term exactly for  $j_{mn} = 0$ . In this limit, all response functions, Eqs. (A1) to (A4), can be exactly reproduced by the corresponding master equations. In the following sections, we will treat the case of  $j_{mn} \neq 0$ , for the case of the second order response, i.e. we will derive equations of motion for the reduced density matrix using the projector  $\mathcal{P}_\tau$ . The application of this approach to the full response function will be treated elsewhere. An alternative to the projector approach is to attempt to derive specific equations of motion for each response function as a whole in a specific perturbation scheme, e.g. second order convolutionless QME (CL-QME) as in Ref. [48]. While both approaches should lead to similar results, the projection operator technique is not limited to any specific way of expanding the equations of motion in terms of system-bath coupling, and we believe it is therefore somewhat more flexible.

#### IV. SECOND ORDER RESPONSE TO LIGHT

The second order optical response can yield an optical signal on the sum or difference frequencies of the exciting

field. Here, we consider only the degenerate experiment when the excitation field have the same frequency, and we are interested in particular in the zero frequency part of the response which does not generate an optical signal. Unlike in spectroscopy where we study a quantum mechanical expectation value (polarization or field), here we would like to study the state of the system achieved by the excitation. Correspondingly, the second order response will not be expressed in terms of response function, but rather in terms of some response operators. By the ‘‘system’’ we mean electronic DOF, and thus the response operators correspond to the reduced density matrix of the system in the same way the response function corresponds to an expectation value of e.g. polarization.

##### A. Excited State of a Molecular System

Assuming that we excited the system by some external field  $E(t)$ , the second order reduced density operator of the system reads as

$$\begin{aligned} \hat{\rho}^{(2)}(t) &= - \int_0^\infty dt_1 \int_0^\infty dt_2 \text{tr}_B \{ \mathcal{U}(t_2) \mathcal{V} \\ &\times \mathcal{U}(t_1) \mathcal{V} w_{\text{eq}} |g\rangle \langle g| \} E(t-t_2) E(t-t_2-t_1). \end{aligned} \quad (27)$$

The excited state part of the second order density operator  $\hat{\rho}^{(2)}$  then yields

$$\begin{aligned} \rho^{(2)}(t) &= \\ &\int_0^\infty dt_1 \int_0^\infty dt_2 \left[ R_I(t_2, t_1) A^*(t-t_2) A(t-t_2-t_1) e^{i\omega t_1} \right. \\ &\left. + R_{II}(t_2, t_1) A(t-t_2) A^*(t-t_2-t_1) e^{-i\omega t_1} \right], \end{aligned} \quad (28)$$

where

$$\begin{aligned} R_I(t_2, t_1) &= \text{Tr}_B \left\{ \mathcal{U}^{(eeee)}(t_2) \right. \\ &\left. \times \mathcal{V}^{(eeeg)} \mathcal{U}^{(egeg)}(t_1) \mathcal{V}^{(eggg)} w_{\text{eq}} |g\rangle \langle g| \right\}, \end{aligned} \quad (29)$$

and

$$\begin{aligned} R_{II}(t_2, t_1) &= \text{Tr}_B \left\{ \mathcal{U}^{(eeee)}(t_2) \right. \\ &\left. \times \mathcal{V}^{(egeg)} \mathcal{U}^{(gege)}(t_1) \mathcal{V}^{(gegg)} w_{\text{eq}} |g\rangle \langle g| \right\}, \end{aligned} \quad (30)$$

are the second order response operators. In Eq. (28) we introduced the electric field envelopes  $A(t)$  and the carrier frequency  $\omega$  so that  $E(t) = A(t)e^{-i\omega t} + c.c.$ . The

interaction of the molecular system with arbitrary light can be expressed using the operators  $R_I$  and  $R_{II}$  as discussed in Ref. [50]. For a general state of the light  $|\psi_{\text{rad}}\rangle$ , the terms  $A^*(t-t_2)A(t-t_2-t_1)e^{i\omega t_1}$  have to be replaced by the light correlation function  $I(t-t_2, t-t_2-t_1) = \langle \psi_{\text{rad}} | \hat{E}^\dagger(t-t_2)\hat{E}(t-t_2-t_1) | \psi_{\text{rad}} \rangle$ , where  $\hat{E}(t)$  is the operator of the electric field in Heisenberg representation. This allows us to calculate the state of a system excited by light with arbitrary properties.

In this paper, we will concentrate on the situation when the molecular system is excited by two ultra-short laser pulses traveling in two different directions  $\mathbf{k}_1$  and  $\mathbf{k}_2$  of which the second one arrives with a delay  $\tau$ . Thus we have  $A_1(t) = A_0 e^{i\mathbf{k}_1 \cdot \mathbf{r}} \delta(t+\tau)$ ,  $A_2(t) = A_0 e^{i\mathbf{k}_2 \cdot \mathbf{r}} \delta(t)$ . The time zero is set to the center of the second pulse. This corresponds to a typical situation in the coherent non-linear spectroscopy, and the time  $t$  in which the excited state evolves corresponds to the population time  $T$  of the non-linear spectroscopy. Inserting the delta function envelopes into Eq. (28) and assuming that the pulse with wave-vector  $\mathbf{k}_1$  precedes the pulse with wave-vector  $\mathbf{k}_2$ , we arrive at

$$\hat{\rho}_I^{(2)}(t; \tau) = R_I(t, \tau) |A_0|^2. \quad (31)$$

This operator corresponds to the excited state time evolution in the left hand side (l.h.s.) diagram of Fig. 2B. The base of this diagram corresponds to the so-called rephasing pathways. When the pulse sequence is reverted (pulse  $\mathbf{k}_1$  arrives second with delay  $\tau$ ) we obtain so-called non-rephasing pathways and the time evolution corresponds to the operator

$$\hat{\rho}_{II}^{(2)}(t; \tau) = R_{II}(t, \tau) |A_0|^2. \quad (32)$$

It is easy to verify that  $\hat{\rho}_I^{(2)}(t; \tau)$  and  $\hat{\rho}_{II}^{(2)}(t; \tau)$  do not have to be Hermitian, and they alone cannot be said to represent a state of a molecular system. This is the result of them being only a portion of the perturbation expansion of the non-linear response operator. Only the sum of Eqs. (29) and (30) yields a Hermitian operator which can describe excited state of a molecular system. This situation has an analogy in the case of 2D coherent spectroscopy where the rephasing and non-rephasing signals alone cannot be interpreted as representing absorption and emission events, while the sum spectrum can be assigned this interpretation [13]. When the system is excited by a single finite length pulse, the two contributions to the excited state are equally weighted, guaranteeing thus the proper properties of the corresponding density matrix.

In the following section we will discuss the equations of motion for  $\hat{\rho}_I^{(2)}(t; \tau)$  and  $\hat{\rho}_{II}^{(2)}(t; \tau)$  to assess the influence of the delay  $\tau$  on the dynamics of their diagonal (populations) and off-diagonal (coherence) elements. We will thus attempt to answer the question whether in the non-linear spectroscopic methods, such as 2D coherent spectroscopy, we observe the expected excited state dynamics, i.e. the one unaffected by the delay  $\tau$ .

## B. Simulation of the Response by Reduced Density Matrix Equations

In order to calculate the second order non-linear response, we need to evaluate the component expressions of Eq. (30). We start with equations of motion for the perturbation of the total density matrix  $W(t)$ . We define the first order operator as

$$W_{II}^{(1)}(t) = \mathcal{U}^{(gege)}(t) \mathcal{V}^{(gegg)} w_{\text{eq}} |g\rangle \langle g|. \quad (33)$$

This operator corresponds to the evolution after the first interaction of the system with light in response function, Eq. (30). The response function has to be read from left to right. The operator  $W_{II}^{(1)}(t)$  satisfies the following equation

$$\frac{\partial}{\partial t} W_{II}^{(1)}(t) = -i\mathcal{L}^{(gege)} W_{II}^{(1)}(t), \quad (34)$$

with the initial condition  $W_{II}^{(1)}(t=0) = \mathcal{V}^{(gegg)} w_{\text{eq}} |g\rangle \langle g| = w_{\text{eq}} |g\rangle \langle g| \mu^{(ge)}$ . RDM equation of motion can be found applying standard AK projection operator, Eq. (22), for which  $(1 - \mathcal{P}_0)W_{II}^{(1)}(t=0)$  is equal to zero identically. The procedure of the derivation of the RDM equation of motion leads to

$$\frac{\partial}{\partial t} \rho_{II}^{(1)}(t) = -i\bar{\mathcal{L}}_0^{(gege)} \rho_{II}^{(1)}(t) - \mathcal{R}_0^{(gege)}(t) \rho_{II}^{(1)}(t), \quad (35)$$

where  $\bar{\mathcal{L}}_0^{(gege)}$  is the coherence block of the electronic Liouville superoperator, and  $\mathcal{R}_0^{(gege)}(t)$  is some second order dephasing tensor. The particular form of  $\mathcal{R}_0^{(gege)}$  depends on the approximations and the theory applied. For a pure dephasing model and a harmonic bath, the dephasing tensor which follows from a second order CL-QME (see e.g. [46]) can be shown to yield an exact dynamics for  $\rho_{II}^{(1)}(t)$  [47]. In secular approximation, Eq. (35) yields

$$\frac{\partial}{\partial t} \rho_{II, \tilde{k}g}^{(1)}(t) = -i\omega_{\tilde{k}g} \rho_{II, \tilde{k}g}^{(1)}(t) - \int_0^t d\tau C_{\tilde{k}\tilde{k}}(\tau) \rho_{II, \tilde{k}g}^{(1)}(t), \quad (36)$$

which is a set of independent equations for optical coherences. Note that we use index  $\tilde{k}$  to denote the excitonic representation. In the limit of  $j_{mn} \rightarrow 0$  (pure dephasing) the states  $|\tilde{k}\rangle$  and  $|k\rangle$  coincide.

The evolution in the second propagation interval can be expressed through the density operator

$$W_{II}^{(2)}(t; \tau) = \mathcal{U}^{(eeee)}(t) \mathcal{V}^{(eeeg)} W_{II}^{(1)}(\tau), \quad (37)$$

which satisfies

$$\frac{\partial}{\partial t} W_{II}^{(2)}(t; \tau) = -i\mathcal{L}^{(eeee)} W_{II}^{(2)}(t; \tau), \quad (38)$$

with the initial condition  $W_{II}^{(2)}(t=0; \tau) = \mathcal{V}^{(eege)} W_{II}^{(1)}(\tau) = \mu^{(eg)} W_{II}^{(1)}(\tau)$ . The application of the

AK projector would lead to a loss of information in the construction of the response function, because the term  $\mathcal{Q}_0\mu^{(eg)}W^{(1)}(\tau) = (1 - \mathcal{P}_0)W^{(1)}(\tau) \neq 0$ . Consequently, even if we successfully derive an exact master equation for  $\rho_{II}^{(2)}(t) = \text{Tr}_B\{W_{II}^{(2)}(t)\}$ , the response function constructed from this equation would be missing the  $\mathcal{Q}$ -containing terms. The parametric projection operator recently suggested in Ref. [49] has the property of eliminating the initial term approximately,  $(1 - \mathcal{P}_\tau)\mu_{eg}W_{II}^{(1)}(\tau) \approx 0$ . In the case of pure dephasing, it turns to zero exactly. We can therefore write an equation of motion for  $\rho_{II}^{(2)}$  which is analogical to Eq. (35)

$$\begin{aligned} \frac{\partial}{\partial t}\rho_{II}^{(2)}(t; \tau) &= -i\bar{\mathcal{L}}_\tau^{(eeee)}\rho_{II}^{(2)}(t; \tau) \\ &- \mathcal{R}_\tau^{(eeee)}(t)\rho_{II}^{(2)}(t; \tau). \end{aligned} \quad (39)$$

Again, the  $\bar{\mathcal{L}}_\tau^{(eeee)}$  is the electronic Liouville superoperator and  $\mathcal{R}_\tau^{(eeee)}(t)$  is the superoperator describing the electronic energy relaxation and the electronic coherence dephasing in the single-exciton band. In the following section, we will derive the relaxation tensor  $\mathcal{R}_\tau^{(eeee)}(t)$  corresponding to the projection operator  $\mathcal{P}_\tau$ .

## V. MASTER EQUATIONS WITH PARAMETRIC PROJECTOR

In this section, we will apply the well-known Nakajima-Zwanzig identity in the second order in system bath interaction Hamiltonian together with the parametric projection operator proposed in Ref. [49]. We are interested in the second interval of the non-linear response, and in the evolution in the single exciton band in particular.

### A. The Choice of Projector

The projector  $\mathcal{P}_\tau$  is chosen in such way that it contains time evolution of the bath in the first interval of the response, where the relevant system dynamics is the one of an optical coherence. The projector corresponding to the pathway  $R_{II}$  and the length of the first interval  $\tau$  reads according to Ref. [49]

$$\mathcal{P}_{\tau, II}\bullet = \text{tr}_B\{\bullet\} U^g(\tau)w_{\text{eq}} \sum_{\bar{n}} U_{\bar{n}}^{e\dagger}(\tau) K_{\bar{n}} e^{g_{\bar{n}\bar{n}}^*(\tau)}. \quad (40)$$

This choice gives an exact description of the bath for  $j_{mn} = 0$ . For a non-zero coupling it corresponds to the secular approximation in the first interval equation of motion, Eq. (36). Further on in the text, all derivations will be done for the pathway  $R_{II}$ , and we omit the index  $II$ . The treatment of the pathway  $R_I$  is analogical. We define evolution operators describing the dynamics of the environmental DOF while the system is in its electronic ground state

$$U^g(\tau) = \exp\left(-\frac{i}{\hbar}(T + \Phi^g)\tau\right), \quad (41)$$

and in the excited eigenstate  $|\bar{n}\rangle$

$$U_{\bar{n}}^e(\tau) = \exp\left(-\frac{i}{\hbar}(T + \Phi_{\bar{n}\bar{n}}^e - \langle\Phi_{\bar{n}\bar{n}}^e - \Phi^g\rangle)\tau\right). \quad (42)$$

By the choice of the projector, Eq. (40), we prescribe an ansatz

$$W^{(2)}(0) = W^{(1)(I)}(\tau) \equiv \rho^{(1)(I)}(\tau)w_\tau^{(I)}, \quad (43)$$

where

$$w_\tau^{(I)} \equiv \sum_{\bar{n}} K_{\bar{n}} U^g(\tau)w_{\text{eq}} U_{\bar{n}}^{e\dagger}(\tau) e^{g_{\bar{n}\bar{n}}^*(\tau)}. \quad (44)$$

For zero resonance coupling  $j_{mn}$ , this is an exact prescription for the bath. For non-zero resonance coupling, it is an approximation comparable to the secular approximation. Projector, Eq. (40), can be written in short as

$$\mathcal{P}_\tau\bullet = \text{tr}_B\{\bullet\}w_\tau^{(I)}. \quad (45)$$

It is important to note that  $w_\tau^{(I)}$  is not a purely bath operator, and it does not generally commute with  $\rho$ . Also the interaction picture with respect to the system Hamiltonian  $H_S$  denoted by  $(I)$  applies to it. It stands on the right hand side (r.h.s.) of  $\rho$  when evaluating  $R_{II}$ , while in  $R_I$  it would stand on the l.h.s. of  $\rho$ . This follows from the diagrams in Fig. 2B. The full form of  $W^{(1)}(\tau)$  is

$$W^{(1)}(\tau) = U^g(\tau)w_{\text{eq}} \times \sum_{\bar{n}} U_{\bar{n}}^{e\dagger}(\tau) K_{\bar{n}} e^{i(\varepsilon_{\bar{n}} + \langle\Phi_{\bar{n}\bar{n}}^e - \Phi^g\rangle)\tau/\hbar} \rho^{(1)}(0). \quad (46)$$

From now on, the upper index (2) will be omitted in text for the sake of brevity.

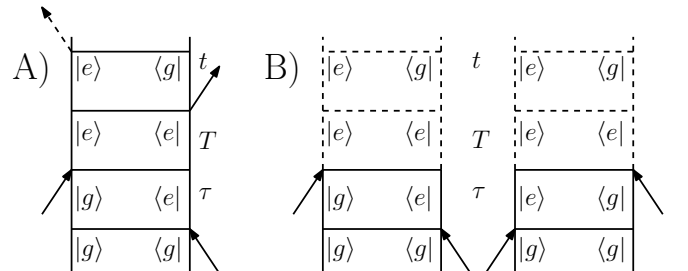


Figure 2: Double-sided Feynman diagrams of the third and the second order response. Part A: The Feynman diagram of the Liouville pathway  $R_2$ . Part B: In full lines, the Feynman diagrams of the response operators  $R_{II}$  (left) and  $R_I$  (right). The dashed part completes the diagram into a corresponding third order response.

We can verify that the projector property  $\mathcal{P}_\tau^2 = \mathcal{P}_\tau$  is fulfilled

$$\begin{aligned} & \mathcal{P}_\tau \mathcal{P}_\tau (|\tilde{m}\rangle\langle\tilde{n}|w) \\ &= |\tilde{m}\rangle\langle\tilde{n}| \text{tr}_B \left\{ U^g(\tau) w_{\text{eq}} U_n^{e\dagger}(\tau) \right\} \text{tr}_B \{w\} e^{2g_{\tilde{n}\tilde{n}}^*(\tau)} \\ &= |\tilde{m}\rangle\langle\tilde{n}| e^{-g_{\tilde{n}\tilde{n}}^*(\tau)} \text{tr}_B \{w\} e^{2g_{\tilde{n}\tilde{n}}^*(\tau)} = \mathcal{P}_\tau (|\tilde{m}\rangle\langle\tilde{n}|w). \end{aligned} \quad (47)$$

Here, we used expression for the line shape function  $g(t)$  in the second cumulant approximation

$$e^{-g(t)} = \text{tr}_B \left\{ U^{g\dagger}(t) U^e(t) w_{\text{eq}} \right\}. \quad (48)$$

The action of the projector  $\mathcal{P}_\tau$  ( $\equiv \mathcal{P}_{\tau,II}$ ) on the electronic state is asymmetric, because the projector was derived for the Liouville pathway II (see Fig 2B).

## B. Parametric Master Equation

Now, we apply the projector  $\mathcal{P}_\tau$ , Eq. (45), to the Nakajima-Zwanzig identity in the interaction picture

$$\begin{aligned} \frac{\partial}{\partial t} \mathcal{P}_\tau W^{(I)}(t) &= \text{NZ}_1 + \text{NZ}_2 + \text{NZ}_3 = \\ & - \mathcal{P}_\tau \mathcal{L}^{(I)}(t) \exp \left( -i \int_{t_0}^t d\tau' \mathcal{Q}_\tau \mathcal{L}^{(I)}(\tau') \mathcal{Q}_\tau \right) \mathcal{Q}_\tau W(t_0) \\ & - \int_0^{t-t_0} d\tau' \left[ \mathcal{P}_\tau \mathcal{L}^{(I)}(t) \exp \left( -i \int_{t_0}^{\tau'} d\tau'' \mathcal{Q}_\tau \mathcal{L}^{(I)}(\tau'') \mathcal{Q}_\tau \right) \right. \\ & \left. \times \mathcal{Q}_\tau \mathcal{L}^{(I)}(t-\tau') \mathcal{P}_\tau W^{(I)}(t-\tau') \right] \\ & - i \mathcal{P}_\tau \mathcal{L}^{(I)}(t) \mathcal{P}_\tau W^{(I)}(t). \end{aligned} \quad (49)$$

We will use Eq. (49) up to the second order in  $\mathcal{L}^{(I)}$ , and we set  $t_0 = 0$ . The term  $\text{NZ}_1$  corresponds to so-called initial term, which we made equal to zero by the choice of the projector. The last term  $\text{NZ}_3$  corresponds to an effective Liouvillian, and it is usually a purely electronic operator. Now, with the parametric projector it contains additional terms originating from the system bath interaction. Its purely electronic part will stand for the effective Liouvillian  $\tilde{\mathcal{L}}_\tau^{(eeee)}$  in Eq. (39), while its additional  $\tau$ -depending contribution we will add to the relaxation tensor  $\mathcal{R}_\tau^{(eeee)}$ . Finally, the term  $\text{NZ}_2$  is a starting point for the derivation of the second order relaxation term, which has a form of a convolution between the RDM and some memory kernel. In the second order expansion of Eq. (49) and with an approximation  $W^{(I)}(t-\tau') \approx W^{(I)}(t)$ , the resulting equation for  $\mathcal{P}_\tau W^{(I)}(t)$  coincides with the second order approximation of the equivalent time-convolutionless identity [56]. Thus the  $\text{NZ}_2$  will lead to a contribution to the tensor  $\mathcal{R}_\tau^{(eeee)}$

in Eq. (39). However, the parametric projection operator technique allows us to keep the convolution form of the equation if it is desired. While the convolution form may have some advantages over the CL-QME [46], only the CL-QME leads in the limit of  $j_{mn} = 0$  to a result coinciding with the one obtained by the second cumulant treatment of the non-linear response functions (see e.g. Ref. [49] and the Appendix D)

Let us point out the most important aspect of the application of the projector  $\mathcal{P}_\tau$  with the identity, Eq. (49). It is important to note that the projector  $\mathcal{P}_\tau$  itself contains the system-bath interaction to all orders in the form of the exponential of the line-shape function (see Eq. (40)). The success of the second order master equations (of the form  $\dot{\rho} = -\alpha_2 \rho$ , where the dot denotes the time derivative, and  $\alpha_2$  is some second order operator) lies in the fact that their solutions includes all orders of the perturbation ( $\rho = e^{-\alpha_2 t} \rho_0$ ). The solution corresponds to a partial summation of the perturbative series to infinity. For some types of bath, such as the bath consisting of harmonic oscillators, this may even lead to exact master equations [47]. When higher order terms are added to the right hand side of the equation motion by a procedure that does not respect the form of higher order terms dictated by the Nakajima-Zwanzig identity, the resulting equation of motion may lead to unphysical results. Therefore, one has to take care in application of the projector  $\mathcal{P}_\tau$ , not to allow higher than second order contributions to appear on the right hand side of Eq. (49). Since the difference between projectors  $\mathcal{P}_0$  and  $\mathcal{P}_\tau$  is only in dynamics of the system-bath coupling during time  $\tau$ , their difference is at least of the first order in  $\Delta\Phi$ . Since the  $\text{NZ}_2$  with AK projector is already of the second order in  $\Delta\Phi$  in all its terms, the difference caused by using projector  $\mathcal{P}_\tau$  will be of higher order in  $\Delta\Phi$ . In the second order master equation, the term  $\text{NZ}_2$  with projector  $\mathcal{P}_\tau$  has to be equivalent to the form obtained from with AK projector (see e.g. [52]). Applying the following approximation  $\rho^{(I)}(t-\tau') \approx \rho^{(I)}(t)$  in the term  $\text{NZ}_2$  we obtain it in the form the second order relaxation term of CL-QME [56].

The details of the evaluation of the term  $\text{NZ}_3$  are presented in Appendix B. As expected it yields a  $\tau$ -dependent term. Putting all results together and tracing over bath DOF we obtain



$$\begin{aligned}
\frac{\partial}{\partial t}\rho^{(I)}(t;\tau) = & \sum_{mn} \int_0^t ds \left[ \right. \\
& - \ddot{g}_{mn}(s)K_m(t)K_n(t-s)\rho^{(I)}(t) \\
& + \ddot{g}_{mn}^*(s)K_m(t)\rho^{(I)}(t)K_n(t-s) \\
& + \ddot{g}_{mn}(s)K_n(t-s)\rho^{(I)}(t)K_m(t) \\
& \left. - \ddot{g}_{nm}^*(s)\rho^{(I)}(t)K_n(t-s)K_m(t) \right] \\
& + \sum_{m\bar{k}} \left( K_m(t)\rho^{(I)}(t)K_{\bar{k}} - \rho^{(I)}(t)K_{\bar{k}}K_m(t) \right) \\
& \times \left( \dot{g}_{m\bar{k}}^*(t+\tau) - \dot{g}_{m\bar{k}}^*(t) \right). \quad (50)
\end{aligned}$$

The first five lines of Eq. (50) corresponds to the standard CL-QME, while the last two lines represent the  $\tau$ -dependent contribution which the standard CL-QME does not predict.

Let us investigate the  $\tau$ -dependent term only. First, we turn to Schrödinger picture by substituting  $\rho^{(I)}(t) = U_S^\dagger(t)\rho(t)U_S(t)$ . We denote the new  $\tau$ -dependent term of the CL-QME by  $\mathcal{D}(t;\tau)$

$$\begin{aligned}
\mathcal{D}(t;\tau)\rho(t) = & \sum_{m\bar{k}} \left( K_m(t)\rho(t)K_{\bar{k}} - \rho(t)K_{\bar{k}}K_m(t) \right) \\
& \times \left( \dot{g}_{m\bar{k}}^*(t+\tau) - \dot{g}_{m\bar{k}}^*(t) \right). \quad (51)
\end{aligned}$$

It can be easily verified that the new term preserves the trace of  $\rho(t)$ , because  $\text{Tr}(K_m(t)\rho(t)K_{\bar{k}} - \rho(t)K_{\bar{k}}K_m(t)) = 0$ . From the inspection of the term  $\dot{g}_{m\bar{k}}^*(t+\tau) - \dot{g}_{m\bar{k}}^*(t)$  we can conclude that the effect of the parameter  $\tau$  is transient. If EGCf tends to zero on a time scale given by some bath correlation time, this term also tends to zero. The dynamics at long times is therefore not affected by the delay between the two excitation interactions. In Appendix C we derived the difference term, Eq. (51), of a special case of molecular homodimer with bath fluctuations uncorrelated between the sides. We found the  $\tau$ -dependent term to be identically equal to zero in this case. In the next section we study the effect of the  $\tau$ -dependent term numerically for a heterodimer.

## VI. NUMERICAL RESULTS AND DISCUSSION

In this section, we study the dynamics of the elements of the response functions, Eqs. (29) and (30). The RDM  $\rho(t;\tau)$  for which we derived Eq. (50) corresponds the response function  $R_{II}$  (see Eq. (32) for the case of  $A_0 = 1$ ). We compare the dynamics in two cases. In the first case, the evolution operator  $\mathcal{U}^{(eee)}(T)$  appearing in Eqs. (29) and (30) is calculated by standard time dependent CL-QME derived using AK projector, Eq. (22). In the second case, it is calculated using Eq. (50). We use

the relation  $\rho_{I,ij}(t) = \rho_{II,ji}^*(t)$  between the RDMs from different Liouville pathways.

The most simple system which exhibits  $\tau$ -dependent correction to the standard CL-QME is a molecular heterodimer. In general, it is characterized by orientation and magnitude of its transition dipole moments, the excited state energies  $\varepsilon_1, \varepsilon_2$  of the component molecules, their resonance coupling  $J$  and the properties of the bath. We denote the difference of the excited state energies by  $\Delta \equiv \varepsilon_1 - \varepsilon_2$ , and we set the magnitudes of the transition dipole moments to unity. The initial condition is assumed in a form  $\rho^{(1)}(0) = |g\rangle\langle g|$ . The evolution during the first interval of the response follows Eq. (36). For the calculations presented on Figs. 3, 4 and 5, we choose the anti-parallel orientation of the transition dipole moments, while for the calculation shown on Figs. 6 and 7, we choose the parallel orientation. The temperature is set to  $T = 300$  K in all calculations.

First, let us investigate the sensitivity of the excited

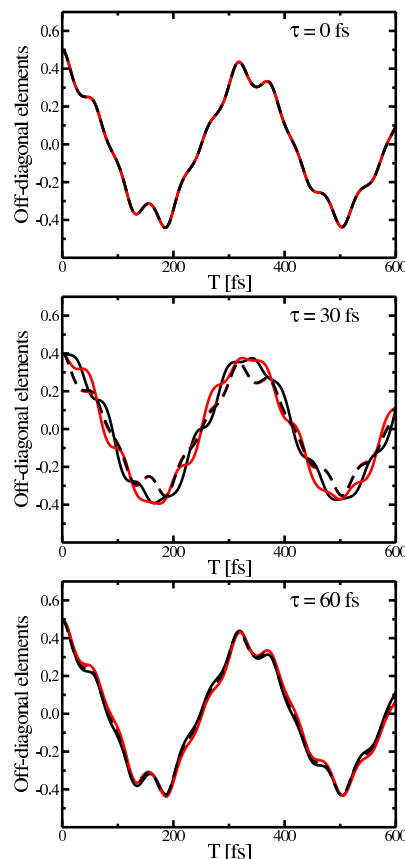


Figure 3: The time evolution of the real parts of  $R_I$  and  $R_{II}$  for a heterodimer with energy gap  $\Delta = 100$   $\text{cm}^{-1}$ , interacting with a bath represented by a general Brownian oscillator with parameters  $\lambda = 50$   $\text{cm}^{-1}$ ,  $\gamma = 1$   $\text{ps}^{-1}$  and  $\Omega_{\text{Bath}} = 100$   $\text{ps}^{-1}$ . Red lines, the matrix element 12 of  $R_I$  according to standard CL-QME (dashed) and the corresponding parametric CL-QME (full). Black lines, the matrix element 12 of  $R_{II}$  according to standard CL-QME (dashed) and the corresponding parametric CL-QME (full).

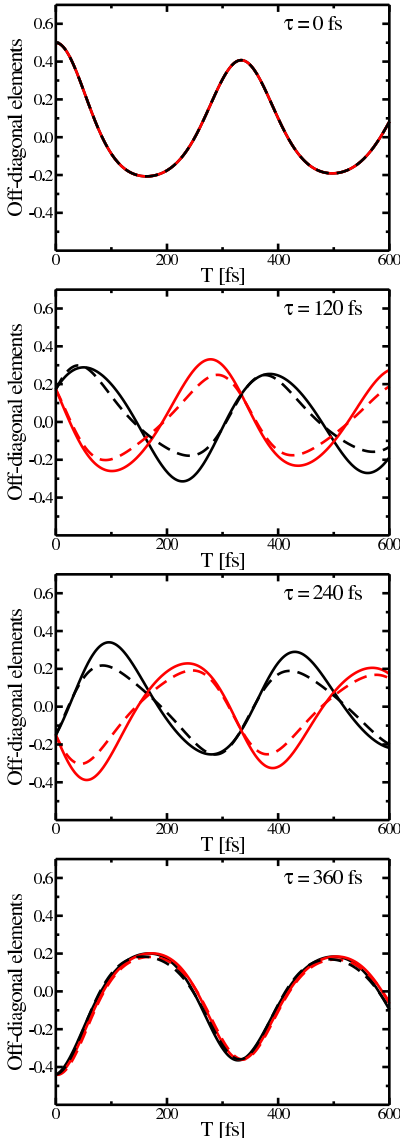


Figure 4: The time evolution of the real parts of  $R_I$  and  $R_{II}$  for a heterodimer with energy gap  $\Delta = 100 \text{ cm}^{-1}$ , interacting with a bath represented by a general Brownian oscillator with parameters  $\lambda = 5 \text{ cm}^{-1}$ ,  $\gamma = 1 \text{ ps}^{-1}$  and  $\Omega_{\text{Bath}} = 19 \text{ ps}^{-1}$ . Red lines, the matrix element 12 of  $R_I$  according to standard CL-QME (dashed) and the corresponding parametric CL-QME (full). Black lines, the matrix element 12 of  $R_{II}$  according to standard CL-QME (dashed) and the corresponding parametric CL-QME (full).

state dynamics to the interplay of the delay  $\tau$  and the phase of the bath vibrations. Fig. 3 shows the dynamics of the electronic coherence between the excited states  $|e_1\rangle$  and  $|e_2\rangle$  in presence of the bath represented by a single-mode general Brownian oscillator with parameters  $\lambda = 50 \text{ cm}^{-1}$ ,  $\gamma = 1 \text{ ps}^{-1}$ ,  $\Omega_{\text{Bath}} = 100 \text{ ps}^{-1}$  and  $\Delta = 100 \text{ cm}^{-1}$ . Both calculations show that the standard CL-QME calculation of  $\mathcal{U}^{(eeee)}(T)$  is insensitive to the phase of bath vibration mode during the time evolution in the first interval. The parametric CL-QME, Eq.

(50), shows a distinct sensitivity to this phase. In both cases, the resonance coupling  $J$  is chosen to be zero, and the dynamics can therefore be evaluated exactly by the cumulant expansion technique (see Appendix D). The numerical evaluation using Eq. (50) indeed matches the analytical result. In the calculation on the Fig. 3, the vibration of the bath is much faster than the period (333 fs) of the electronic coherence. The two theories give the same result for  $\tau = 0 \text{ fs}$ , then they start to deviate and after one period of bath oscillator, at  $\tau = 60 \text{ fs}$ , they coincide again. Initial phase of  $\rho_{I,12}$  and  $\rho_{II,12}$  is in general different at  $T = 0 \text{ fs}$  because of their different time evolution in the first interval (they are not simply complex conjugates of each other). In the Fig. 4, we calculated the same system, but we used bath with parameters  $\lambda = 5 \text{ cm}^{-1}$ ,  $\gamma = 1 \text{ ps}^{-1}$ ,  $\Omega_{\text{Bath}} = 19 \text{ ps}^{-1}$ . The frequency is now resonant with the frequency of the electronic coherence, which makes the effect more significant. The two theories give the same result for  $\tau = 0 \text{ fs}$ , and at  $\tau = 360 \text{ fs}$ , which is approximately one period of the bath vibration mode. Unlike in Fig.3, the initial phase of  $\rho_{I,12}$  and  $\rho_{II,12}$  differs significantly in  $T = 0 \text{ fs}$  because of their different time evolution in  $\tau$ .

In both the cases studied above, the time evolution of the off-diagonal elements of the second order response operator is slightly modulated by the time evolution of the vibrational DOF. The phase of the oscillations seems to be mostly unaffected.

Figs. 5 and 6 demonstrate the influence of the resonance coupling on the population and electronic coherence dynamics in the homodimer. As above, we perform calculation according to standard CL-QME and the parametric CL-QME. This time, we choose the overdamped Brownian oscillator with fixed  $\tau = 60 \text{ fs}$  and  $\Delta = 100 \text{ cm}^{-1}$ , reorganization energy  $\lambda = 120 \text{ cm}^{-1}$  and correlation time  $\tau_c = \Lambda^{-1} = 50 \text{ fs}$  to represent the bath, and we change the resonance coupling. We calculate both diagonal and off-diagonal elements (“populations” and “coherences”) of the operators  $\rho_{I/II}$ . For  $J = 0 \text{ cm}^{-1}$ , there is no population dynamics. By increasing the coupling, the difference between the theories in the diagonal elements increases. In the Fig. 5, the dipole moments of the molecules are anti-parallel, while in Fig. 6 they are parallel.

Let us now investigate a molecular dimer coupled to overdamped harmonic bath and to a single harmonic mode with frequency  $\Omega_{\text{Bath}}$ . The harmonic mode is assumed to continue oscillating even long after thermalization in the overdamped part of the bath has taken place. Therefore, the  $\tau$ -dependent term of Eq. (51) changes the system dynamics also at long times. The time dependence of the density operator elements for different  $\tau$  is shown in Fig. 7. Parameters of the overdamped bath are  $\Lambda^{-1} = 100 \text{ fs}$  and  $\lambda_{\text{overdamped}} = 12 \text{ cm}^{-1}$  and of the harmonic mode  $\lambda_{\text{harmonic}} = 30 \text{ cm}^{-1}$ ,  $\Omega_{\text{Bath}} = 60 \text{ cm}^{-1}$ . The dimer is characterized by  $\Delta = 100 \text{ cm}^{-1}$ ,  $J = 33.1 \text{ cm}^{-1}$  and the parallel electronic transition dipole moments of the molecules. We can notice that the interaction of the

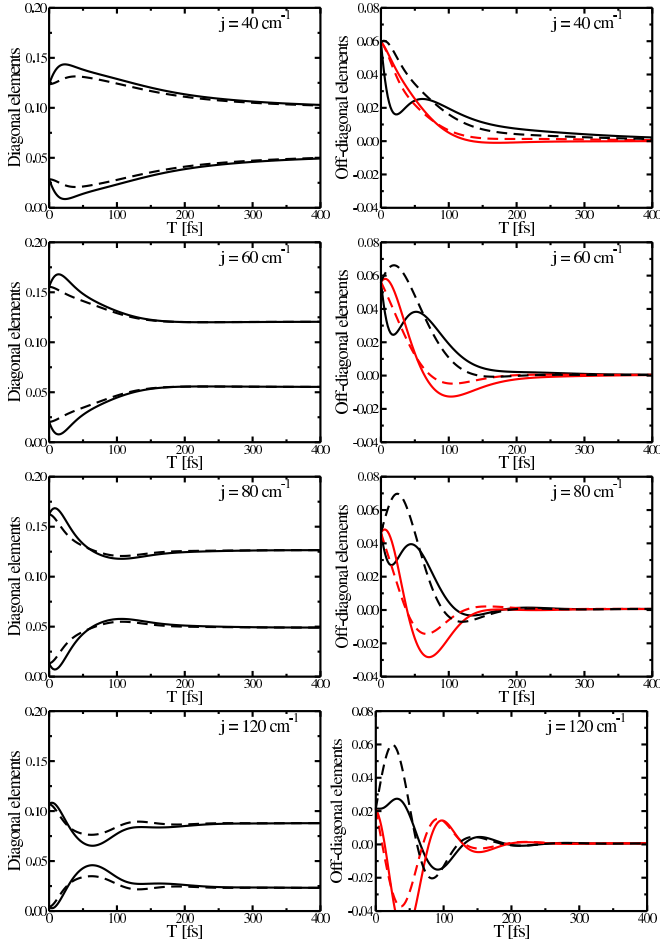


Figure 5: The time evolution of the real parts of  $R_I$  and  $R_{II}$  and their dependency on the resonance coupling  $j$  for a heterodimer with energy gap  $\Delta = 100 \text{ cm}^{-1}$  and an anti-parallel arrangement of the transition dipole moments, interacting with a bath represented by an overdamped Brownian oscillator with reorganization energy  $\lambda = 120 \text{ cm}^{-1}$  and correlation time  $\tau_c = \Lambda^{-1} = 50 \text{ fs}$ . The delay between the two pulses is fixed to  $\tau = 60 \text{ fs}$ . Black lines, the matrix elements 11, 22 (left column) and 12 (right column) of  $R_{II}$  according to standard CL-QME (dashed) and the corresponding parametric CL-QME (full). Red lines, the matrix element 12 (right column) of  $R_I$  according to standard CL-QME (dashed) and the corresponding parametric CL-QME (full).

vibrational mode with the electronic DOF induces oscillations in both the diagonal and off-diagonal elements of the density operator. The amplitude of the oscillations increases with increasing  $\tau$ . Since the EGCF of the harmonic mode, Eq. (17), is periodic, we expect the relative amplitude of the oscillations to decrease again for sufficiently long  $\tau$ , and to become zero for  $\tau = 2\pi/\Omega_{\text{Bath}}$ . However, in such long  $\tau$  the second order response would be almost zero due to the decay of the optical coherence in the first interval. Fig. 7 suggests that the phase of the oscillation does not change linearly with  $\tau$ . To understand this behavior, we can study a simple equation of the form

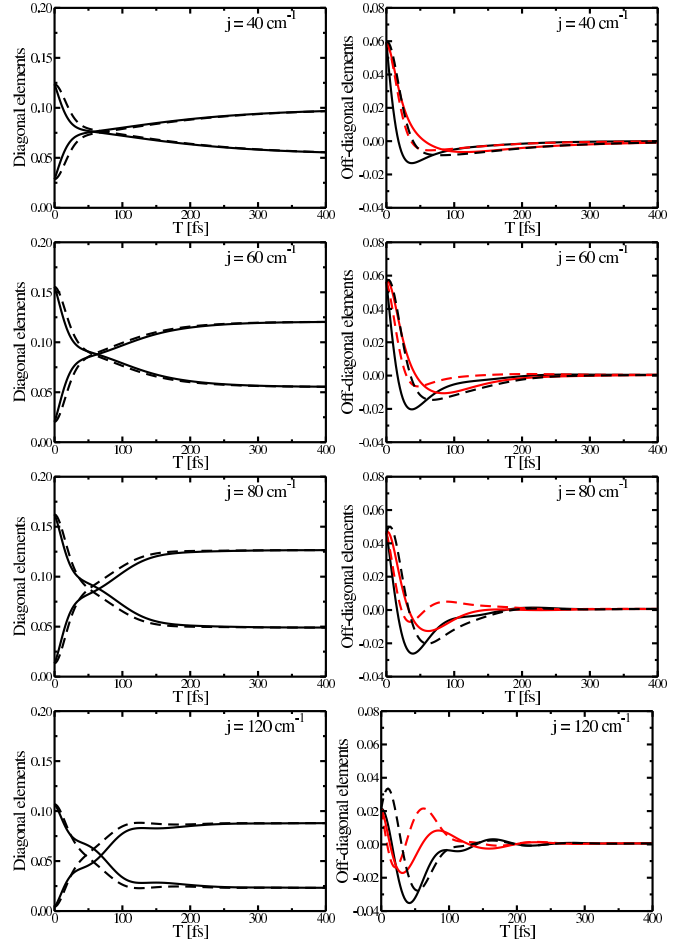


Figure 6: The same as Fig. 5 but for a heterodimer with parallel transition dipole moment arrangement.

$$\dot{\rho}(t) = -\alpha(\rho(t) - \rho_0) + (f(t + \tau) - f(t))\rho(t), \quad (52)$$

which describes exponential decay to a limiting value  $\rho_0$  with the rate constant  $\alpha$  and a modulation by the function

$$f(t) = \int_0^t d\tau A \cos(\omega\tau). \quad (53)$$

Eq. (53) represents a first integral of the EGCF of an underdamped vibrational mode, Eq. (17). The solution of Eq. (53) with the parameters  $\alpha = 0.01$ ,  $A = 10^{-4}$ ,  $\omega^{-1} = 60$  and  $\rho_0 = 0.6$  is shown in Fig. 8. We can see that the oscillation phase and period of the oscillations is indeed not proportional to  $\tau$ , and the amplitude increases with  $\tau$  similarly to Fig. 7. The behavior is therefore a direct consequence of the parametric QME.

The overall picture arising from the numerical simulations is the following: Except for special cases, such as the molecular homodimer, the excited state dynamics of an

open quantum system, as it is observed by the non-linear spectroscopy, indeed depends on the delay  $\tau$  between the FWM scheme. The 2D spectroscopy therefore observes a certain averaged dynamics. The effects seem to be rather small in most cases, but they might be observable by an advanced implementation of 2D spectroscopy. They are especially pronounced in the case of the intramolecular vibrational modes, which have frequency similar to the electronic energy gap between excitonic levels. Both the dynamics of electronic level populations and electronic coherences are affected. In order to identify these effects in the experimental data, the theory has to be extended to include also the third interval of the third order non-linear response. The corresponding projection operator  $\mathcal{P}_{T+\tau}$  which now depends on the duration of both the coherence and the population intervals  $\tau$  and  $T$ , respectively, has been already proposed and tested for  $j_{mn} = 0$  in Ref. [49]. The formulation of the theory for the third interval of the response of a multilevel excitonic system in a similar manner as performed in this paper for the second interval will be the subject of our future work.

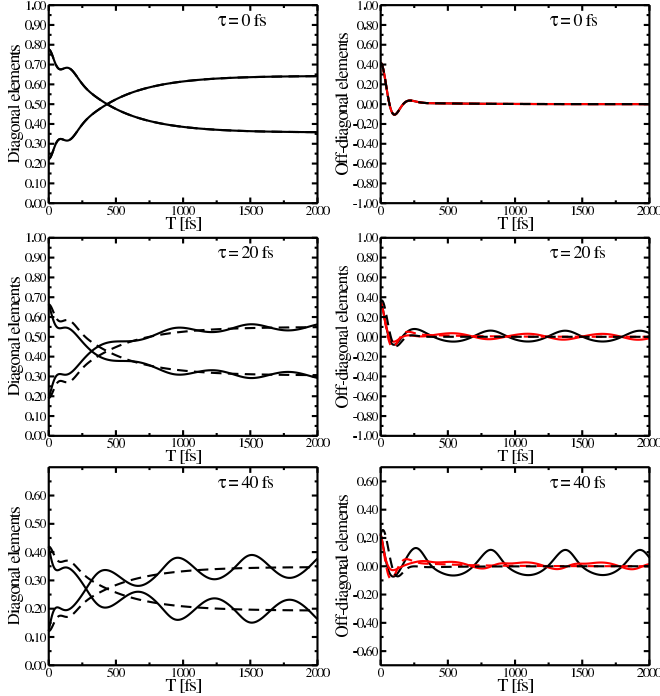


Figure 7: The time evolution of the real parts of  $R_I$  and  $R_{II}$  a heterodimer with energy gap  $\Delta = 100 \text{ cm}^{-1}$ , resonance coupling  $j = 33.1 \text{ cm}^{-1}$  and a parallel arrangement of the transition dipole moments, interacting with a bath represented by one overdamped Brownian oscillator with parameters  $\Lambda^{-1} = 100 \text{ fs}$  and  $\lambda_{\text{overdamped}} = 12 \text{ cm}^{-1}$  and an underdamped vibration with reorganization energy  $\lambda_{\text{harmonic}} = 30 \text{ cm}^{-1}$  and frequency  $\Omega_{\text{Bath}} = 60 \text{ cm}^{-1}$ . Black lines, the matrix elements 11, 22 (left column) and 12 (right column) of  $R_{II}$  according to standard CL-QME (dashed) and the corresponding parametric CL-QME (full). Red lines, the matrix element 12 (right column) of  $R_I$  according to standard CL-QME (dashed) and the corresponding parametric CL-QME (full).

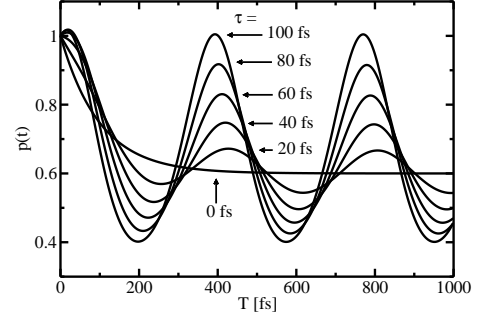


Figure 8: The time evolution of “population” according to model Eq. (52). The curves are solutions for  $\tau$  increasing from 0 fs to 100 fs with step of 20 fs.

## VII. CONCLUSIONS

In this paper, we have demonstrated that the third and the second order non-linear response of a multilevel system cannot be completely evaluated by propagating reduced density matrix by equations of motion derived using a single projection operator. Such treatment would inevitably neglect correlations between the time evolution of the bath during the neighboring intervals of the non-linear response. We have derived equation of motion, the parametric quantum master equation, which takes these correlations into account approximately, and showed that in the absence of resonance coupling the method yields an agreement with the result obtained by the second order cumulant method. We confirm by numerical simulations that for different delays  $\tau$  between the excitation pulses, distinct dynamics of both excite state populations and electronic coherence occurs, in the presence of environmental degrees of freedom with finite bath correlation time and in the presence of intramolecular vibrations. The two-dimensional Fourier transformed spectroscopy sees in these cases some averaged dynamics.

## Acknowledgments

This work was supported by the Czech Science Foundation (GACR) grant nr. 205/10/0989 and the Ministry of Education, Youth and Sports of the Czech Republic via grant KONTAKT ME899 and the research plan MSM0021620835. J. O. acknowledges the support by grant GAUK 102-10/251386.

## Appendix A: Third-Order Non-linear Response Functions

The four standard response functions (so-called Liouville pathways) of a two-band electronic system read in our block formalism as

$$R_1(t, T, \tau) = \text{tr}\{\mu^{(ge)}\mathcal{U}^{(egeg)}(t)\mathcal{V}^{(egee)}\} \\ \times \mathcal{U}^{(eeee)}(T)\mathcal{V}^{(eeeg)}\mathcal{U}^{(egeg)}(\tau)\mathcal{V}^{(eggg)}W_{\text{eq}}^{(gg)}, \quad (\text{A1})$$

$$R_2(t, T, \tau) = \text{tr}\{\mu^{(ge)}\mathcal{U}^{(egeg)}(t)\mathcal{V}^{(egee)}\} \\ \times \mathcal{U}^{(eeee)}(T)\mathcal{V}^{(eege)}\mathcal{U}^{(gege)}(\tau)\mathcal{V}^{(gegg)}W_{\text{eq}}^{(gg)}, \quad (\text{A2})$$

$$R_3(t, T, \tau) = \text{tr}\{\mu^{(ge)}\mathcal{U}^{(egeg)}(t)\mathcal{V}^{(eggg)}\} \\ \times \mathcal{U}^{(gggg)}(T)\mathcal{V}^{(ggge)}\mathcal{U}^{(gege)}(\tau)\mathcal{V}^{(gegg)}W_{\text{eq}}^{(gg)}, \quad (\text{A3})$$

$$R_4(t, T, \tau) = \text{tr}\{\mu^{(ge)}\mathcal{U}^{(egeg)}(t)\mathcal{V}^{(eggg)}\} \\ \times \mathcal{U}^{(gggg)}(T)\mathcal{V}^{(ggeg)}\mathcal{U}^{(egeg)}(\tau)\mathcal{V}^{(eggg)}W_{\text{eq}}^{(gg)}. \quad (\text{A4})$$

Here,  $W_{\text{eq}}^{(gg)} = w_{\text{eq}}|g\rangle\langle g|$  where  $w_{\text{eq}}$  is the bath equilibrium density operator.

## Appendix B: Derivation of Relaxation Terms

In this section we will evaluate the term  $\text{NZ}_3$  of Eq. (49). Applying the definitions of its component operators from Section V we obtain

$$\text{NZ}_3 = -\frac{i}{\hbar}\text{tr}_B\left\{\left[\sum_m \Delta\Phi_m(t)K_m(t), \rho^{(I)}(t)w_\tau^{(I)}\right]_-\right\}w_\tau^{(I)} \quad (\text{B1})$$

where

$$\rho^{(I)}(t) = \text{tr}_B\left\{\mathcal{P}_\tau W^{(I)}(t)\right\}. \quad (\text{B2})$$

Using Eq. (44) yields

$$\text{NZ}_3 = -\frac{i}{\hbar}\sum_{m\bar{k}} e^{g_{\bar{k}}^*(\tau)}\text{tr}_B\left\{\Delta\Phi_m(t)K_m(t)\rho^{(I)}(t)w_{\text{eq}}\right. \\ \times U^g(\tau)U_{\bar{k}}^{e\dagger}(\tau)K_{\bar{k}}\left.\right\}w_\tau^{(I)} \\ + \frac{i}{\hbar}\sum_{m\bar{k}} e^{g_{\bar{k}}^*(\tau)}\text{tr}_B\left\{\rho^{(I)}(t)w_{\text{eq}}U^g(\tau)U_{\bar{k}}^{e\dagger}(\tau)\right. \\ \times K_{\bar{k}}\Delta\Phi_m(t)K_m(t)\left.\right\}w_\tau^{(I)}. \quad (\text{B3})$$

Now we have to set  $e^{g_{\bar{k}}^*(\tau)} \approx 1$  since its contribution is of higher order in  $\Delta\Phi$ . Applying the first order expansion

$$U^g(\tau)U_{\bar{n}}^{e\dagger}(\tau) \approx 1 + \frac{i}{\hbar}\int_0^\tau d\tau' \Delta\Phi_{\bar{n}\bar{n}}(-\tau'), \quad (\text{B4})$$

yields

$$\text{NZ}_3 = -\frac{i}{\hbar}\sum_{m\bar{k}}\text{tr}_B\left\{\Delta\Phi_m(t)K_m(t)\rho^{(I)}(t)w_{\text{eq}}\right. \\ \times \left(1 + \frac{i}{\hbar}\int_0^\tau d\tau' \Delta\Phi_{\bar{k}\bar{k}}(-\tau')\right)K_{\bar{k}}\left.\right\}w_\tau^{(I)} \\ + \frac{i}{\hbar}\sum_{m\bar{k}}\text{tr}_B\left\{\left(1 + \frac{i}{\hbar}\int_0^\tau d\tau' \Delta\Phi_{\bar{k}\bar{k}}(-\tau')\right)\right. \\ \times K_{\bar{k}}\Delta\Phi_m(t)K_m(t)\rho^{(I)}(t)w_{\text{eq}}\left.\right\}w_\tau^{(I)}. \quad (\text{B5})$$

Now, we define a line shape function

$$g_{a\bar{b}}(t) = \frac{1}{\hbar^2}\int_0^t d\tau \int_0^\tau \tau' \langle \Delta\Phi_a(\tau')\Delta\Phi_{\bar{b}} \rangle, \quad (\text{B6})$$

where it is noteworthy that one of its indices represents the site- and the other the exciton-basis. The  $\text{NZ}_3$  term can then be expressed as

$$\text{NZ}_3 = \frac{1}{\hbar^2}\int_0^\tau d\tau' \left[ \sum_{m\bar{k}} K_m(t)\rho^{(I)}(t)K_{\bar{k}} - \rho^{(I)}(t)K_{\bar{k}}K_m(t) \right] \\ \times \text{tr}_B\left\{\Delta\Phi_{\bar{k}}(-\tau')\Delta\Phi_m(t)w_{\text{eq}}\right\}w_\tau^{(I)} \\ = \sum_{m\bar{k}} \left( K_m(t)\rho^{(I)}(t)K_{\bar{k}} - \rho^{(I)}(t)K_{\bar{k}}K_m(t) \right) \\ \times \left( \dot{g}_{m\bar{k}}^*(t+\tau) - \dot{g}_{m\bar{k}}^*(t) \right) w_\tau^{(I)}. \quad (\text{B7})$$

In order to obtain the last two lines of Eq. (50) we will trace Eq. (B7) over the bath DOF.

## Appendix C: The $\tau$ -dependent Term for a Homodimer

Let us assume a molecular homodimer with the Hamiltonian

$$H_S = \begin{bmatrix} 0 & j \\ j & 0 \end{bmatrix}, \quad (\text{C1})$$

$$H_{S-B} = \begin{bmatrix} \Delta\Phi_1 & 0 \\ 0 & \Delta\Phi_2 \end{bmatrix}. \quad (\text{C2})$$

This yields in the exciton basis

$$H_S = \begin{bmatrix} -j & 0 \\ 0 & j \end{bmatrix}, \quad (\text{C3})$$

$$H_{S-B} = \frac{1}{2} \begin{bmatrix} \Delta\Phi_1 + \Delta\Phi_2 & \Delta\Phi_2 - \Delta\Phi_1 \\ \Delta\Phi_2 - \Delta\Phi_1 & \Delta\Phi_1 + \Delta\Phi_2 \end{bmatrix}. \quad (\text{C4})$$

The derivative of the line shape function which enters the  $\tau$ -dependent correction  $\mathcal{D}(t; \tau)$  of the CL-QME then reads as

$$\dot{g}_{m\bar{k}}(t) = \frac{1}{2} \int_0^t dt' \sum_{n=1}^2 \langle \Delta\Phi_m(t') \Delta\Phi_n \rangle. \quad (\text{C5})$$

We neglect the cross-terms  $\langle \Delta\Phi_i(t) \Delta\Phi_j \rangle$  for  $i \neq j$ , because we assume only local correlations of the bath. In a homodimer  $\Delta\Phi_1 = \Delta\Phi_2$ , and we get  $\dot{g}_{1\bar{k}}(t) = \dot{g}_{2\bar{k}}(t) = \dot{g}(t)$  from which it follows that

$$\dot{g}_{m\bar{k}}^*(t + \tau) - \dot{g}_{m\bar{k}}^*(t) = \dot{g}^*(t + \tau) - \dot{g}^*(t). \quad (\text{C6})$$

By substituting this equation into Eq. (51), the  $\tau$ -containing term  $\mathcal{D}(t; \tau)$  turns to zero, because

$$\sum_{m\bar{k}} (K_m \rho(t) K_{\bar{k}} - \rho(t) K_{\bar{k}} K_m) = 0. \quad (\text{C7})$$

Thus the  $\tau$ -dependent correction to the CL-QME is zero for the case of a homodimer.

#### Appendix D: Pure Dephasing of an Electronic Coherence

In a pure dephasing model of the system-bath interaction, analytical solution for the dynamics of electronic coherences can be obtained with the cumulant expansion technique. The time evolution of coherence  $\rho_{ee'}^{(2)}(t; \tau)$

reads as

$$\rho_{ee'}^{(2)}(t, \tau) = \text{tr}_B \left\{ U_e(t) U_g(\tau) W_{\text{eq}} U_{e'}^\dagger(\tau) U_{e'}^\dagger(t) \right\} \rho_{ee'}^{(2)}(0), \quad (\text{D1})$$

where we set all transition dipole moments to one. By using the second cumulant procedure [14] we can evaluate the expression into

$$\rho_{ee'}^{(2)}(t; \tau) = e^{-g_{ee}(t) - g_{e'e'}^*(t+\tau) + g_{e'e}(t) + g_{e'e'}^*(t+\tau) - g_{e'e'}^*(\tau)} \rho_{ee'}^{(2)}(0). \quad (\text{D2})$$

Equivalently, we can rewrite Eq. (D2) in form of a master equation

$$\begin{aligned} \frac{d}{dt} \rho_{ee'}^{(2)}(t; \tau) = & \left[ -\dot{g}_{e'e'}^*(t) - \dot{g}_{ee}(t) \right. \\ & + \dot{g}_{e'e}(t) + \dot{g}_{e'e'}^*(t) \\ & - (\dot{g}_{e'e'}^*(t + \tau) - \dot{g}_{e'e'}^*(t)) \\ & \left. + (\dot{g}_{ee}^*(t + \tau) - \dot{g}_{ee}^*(t)) \right] \rho_{ee'}^{(2)}(t; \tau). \quad (\text{D3}) \end{aligned}$$

The first four terms on the right hand side of Eq. (D3) are described by the CL-QME. The remaining terms can be matched with the term  $\mathcal{D}(t; \tau)$  derived in this paper. Eq. (50) therefore gives the correct result for this simple exactly solvable case.

- 
- [1] R. R. Ernst, G. Bodenhausen, and A. Wokaun, *Principles of Nuclear Magnetic Resonance in One and Two Dimensions* (Clarendon Press, Oxford, 2004).
- [2] P. Hamm, M. Lim, and R. M. Hochstrasser, *J. Phys. Chem. B* **102**, 6123 (1998).
- [3] M. C. Asplund, M. T. Zanni, and R. M. Hochstrasser, *Proc. Natl. Acad. Sci. U.S.A.* **97**, 8219 (2000).
- [4] V. Cervetto, J. Helbing, J. Bredenbeck, and P. Hamm, *J. Chem. Phys.* **121**, 5935 (2004).
- [5] M. L. Cowan, J. P. Ogilvie, and R. J. D. Miller, *Chem. Phys. Lett.* **386**, 184 (2004).
- [6] T. Brixner, I. V. Stiopkin, and G. R. Fleming, *Opt. Lett.* **29**, 884 (2004).
- [7] F. Milota, J. Sperling, A. Nemeth, T. Mančal, and H. F. Kauffmann, *Acc. Chem. Res.* **42**, 1364 (2009).
- [8] E. Collini and G. D. Scholes, *Science* **323**, 369 (2009).
- [9] G. S. Engel, T. R. Calhoun, E. L. Read, T.-K. Ahn, T. Mančal, Y.-C. Cheng, R. E. Blankenship, and G. R. Fleming, *Nature* **446**, 782 (2007).
- [10] N. S. Ginsberg, Y.-C. Cheng, and G. R. Fleming, *Acc. Chem. Res.* **42**, 1352 (2009).
- [11] K. W. Stone, K. Gundogdu, D. B. Turner, X. Li, S. T. Cundiff, and K. A. Nelson, *Science* **324**, 1169 (2009).
- [12] S. Mukamel, *Annu. Rev. Phys. Chem.* **51**, 691 (2000).
- [13] D. M. Jonas, *Annu. Rev. Phys. Chem.* **54**, 425 (2003).
- [14] S. Mukamel, *Principles of nonlinear spectroscopy* (Oxford University Press, Oxford, 1995).
- [15] M. H. Cho, H. M. Vaswani, T. Brixner, J. Stenger, and G. R. Fleming, *J. Phys. Chem. B* **109**, 10542 (2005).
- [16] A. V. Pislakov, T. Mančal, and G. R. Fleming, *J. Chem. Phys.* **124**, 234505 (2006).
- [17] P. Kjellberg, B. Bruggemann, and T. Pullerits, *Physical Review B* **74**, 024303 (2006).
- [18] T. Brixner, J. Stenger, H. M. Vaswani, M. Cho, R. E. Blankenship, and G. R. Fleming, *Nature* **434**, 625 (2005).
- [19] E. Collini, C. Y. Wong, K. E. Wilk, P. M. G. Curmi, P. Brumer, and G. D. Scholes, *Nature* **463**, 644 (2010).
- [20] G. Panitchayangkoon, D. Hayes, K. A. Fransted, J. R. Caram, E. Harel, J. Wen, R. E. Blankenship, and G. S. Engel, *PNAS* **107**, 12766 (2010).
- [21] A. Ishizaki and G. R. Fleming, *New Journal of Physics* **12**, 055004 (2010).
- [22] M. Sarovar, A. Ishizaki, G. R. Fleming, and K. B. Whaley, *Nature Physics* **6**, 462 (2010).
- [23] F. Caruso, A. W. Chin, A. Datta, S. F. Huelga, and M. B. Plenio, *Phys. Rev. A* **81**, 062346 (2010).
- [24] M. Mohseni, P. Rebentrost, S. Lloyd, and A. Aspuru-Guzik, *J. Chem. Phys.* **129**, 174106 (2008).
- [25] A. Olaya-Castro, C. F. Lee, F. F. Olsen, and N. F. Johnson, *Phys. Rev. B* **78**, 085115 (2008).

- [26] P. Rebentrost, M. Mohseni, I. Kassal, S. Lloyd, and A. Aspuru-Guzik, *New J. Phys.* **11**, 033003 (2009).
- [27] F. Caruso, A. W. Chin, A. Datta, S. F. Huelga, and M. B. Plenio, *J. Chem. Phys.* **131**, 105106 (2009).
- [28] A. W. Chin, A. Datta, F. Caruso, S. F. Huelga, and M. B. Plenio, *New J. Phys.* **12**, 065002 (2010).
- [29] T. R. Calhoun, N. S. Ginsberg, G. S. Schlau-Cohen, Y.-C. Cheng, M. Ballottari, R. Bassi, and G. R. Fleming, *J. Phys. Chem. B* **113**, 16291 (2009).
- [30] A. Nemeth, F. Milota, T. Mančal, V. Lukevs, H. F. Kauffmann, and J. Sperling, *Chem. Phys. Lett.* **459**, 94 (2008).
- [31] A. Nemeth, F. Milota, T. Mančal, V. Lukeš, J. Hauer, H. F. Kauffmann, and J. Sperling, *J. Chem. Phys.* **132**, 184514 (2010).
- [32] H. van Amerongen, L. Valkunas, and R. van Grondelle, *Photosynthetic Excitons* (World Scientific, Singapore, 2000).
- [33] Y. Tanimura, *J. Phys. Soc. Jpn.* **75**, 082001 (2006).
- [34] A. Ishizaki and G. R. Fleming, *J. Chem. Phys.* **130**, 234111 (2009).
- [35] A. Ishizaki and G. R. Fleming, *J. Chem. Phys.* **130**, 234110 (2009).
- [36] V. Novoderezhkin, M. Wendling, and R. van Grondelle, *J. Phys. Chem. B* **107**, 11534 (2003).
- [37] V. I. Novoderezhkin, M. A. P. and Herbert van Amerongen, and R. van Grondelle, *J. Phys. Chem. B* **109**, 10493 (2005).
- [38] R. van Grondelle and V. I. Novoderezhkin, *Phys. Chem. Chem. Phys.* **8**, 793 (2006).
- [39] D. Abramavičius, B. Palmieri, D. V. Voronine, F. Šanda, and S. Mukamel, *Chemical Reviews* **109**, 2350 (2009).
- [40] D. Zigmantas, E. L. Read, T. Mančal, T. Brixner, A. T. Gardiner, R. J. Cogdell, and G. R. Fleming, *Proceedings of the National Academy of Sciences of the United States Of America* **103**, 12672 (2006).
- [41] E. L. Read, G. S. Engel, T. R. Calhoun, T. Mančal, T. K. Ahn, R. E. Blankenship, and G. R. Fleming, *Proceedings of the National Academy of Sciences of the United States of America* **104**, 14203 (2007).
- [42] H. Rhee, Y.-G. June, J.-S. Lee, K.-K. Lee, J.-H. Ha, Z. H. Kim, S.-J. Jeon, and M. Cho, *Nature* **548**, 310 (2009).
- [43] D. Abramavicius and S. Mukamel, *J. Chem. Phys.* **133**, 064510 (2010).
- [44] W. M. Zhang, T. Meier, V. Chernyak, and S. Mukamel, *J. Chem. Phys.* **108**, 7763 (1998).
- [45] B. Palmieri, D. Abramavicius, and S. Mukamel, *J. Chem. Phys.* **130**, 204512 (2010).
- [46] J. Olšina and T. Mančal, *Journal of Molecular Modelling* **110**, 23456 (2010).
- [47] R. Doll, D. Zueco, M. Wubs, S. Kohler, and P. Hanggi, *Chem. Phys.* **347**, 243 (2008).
- [48] M. Richter and A. Knorr, *Annals of Physics* **325**, 711 (2010).
- [49] T. Mančal and F. Šanda, ArXiv 1011.3803v1 (2011).
- [50] T. Mančal and L. Valkunas, *New Journal of Physics* **12**, 065044 (2010).
- [51] *Chlorophylls and bacteriochlorophylls*, edited by B. Grimm, R. J. Porra, W. Rüdiger, and H. Scheer (Springer, Dordrecht, 2006).
- [52] V. May and O. Kühn, *Charge and Energy Transfer Dynamics in Molecular Systems* (Wiley-VCH, Berlin, 2001).
- [53] P. N. Argyres and P. L. Kelley, *Phys. Rev. A* **134**, 98 (1964).
- [54] M. F. Gelin, D. Egorova, and W. Domcke, *J. Chem. Phys.* **123**, 164112 (2005).
- [55] T. Mančal, A. Pislakov, and G. Fleming, *Journal of Chemical Physics* **124**, 234504 (2006).
- [56] B. Fain, *Irreversibilities in Quantum Mechanics* (Kluwer Academic Publishers, Dordrecht, 2000).